Macromolecular Bioscience
www.mbs-journal.de

Assembly of pH-Responsive Antibody-Drug-Inspired Conjugates

Marco Raabe, Astrid Johanna Heck, Siska Führer, Dominik Schauenburg, Michaela Pieszka, Tao Wang, Maksymilian Marek Zegota, Lutz Nuhn, David Y. W. Ng, Seah Ling Kuan, and Tanja Weil**

With the advent of chemical strategies that allow the design of smart bioconjugates, peptide- and protein-drug conjugates are emerging as highly efficient therapeutics to overcome limitations of conventional treatment, as exemplified by antibody-drug conjugates (ADCs). While targeting peptides serve similar roles as antibodies to recognize overexpressed receptors on diseased cell surfaces, peptide-drug conjugates suffer from poor stability and bioavailability due to their low molecular weights. Through a combination of a supramolecular protein-based assembly platform and a pH-responsive linker, the authors devise herein the convenient assembly of a trivalent protein-drug conjugate. The conjugate should ideally possess distinct features of ADCs such as 1) recognition sites that recognize cell receptor and are arranged on 2) distinct locations on a high molecular weight protein scaffold, 3) a stimuli-responsive linker, as well as 4) an attached payload such as a drug molecule. These AD-like conjugates target cancer cells that overexpress somatostatin receptors, can enable controlled release in the microenvironment of cancer cells through a new pH-responsive biotin linker, and exhibit stability in biological media.

1. Introduction

Biomolecules such as peptides and proteins are emerging as powerful therapeutics due to their ability to interact selectively with biological targets and to effect specific biological responses.[1] One of the most eminent biotherapeutics are antibody-drug conjugates (ADCs) that represent powerful treatment options by integrating the specific recognition of antibodies toward selective cell types with potent cytotoxic drugs that can induce apoptosis.[2] In particular the recent progress in site-selective protein modifications expanded the chemical toolbox to design structurally precise ADCs with improved activities in a reproducible fashion.[3–7] Moreover, the design of tailored linkers connecting the drug molecules with the antibody surface and allowing the controlled release of the drug payload stimulated by physiological environment unique to diseased cells has further increased their efficacy.[8,9] Several ADCs are already in clinical trials, thus underlining their importance and potential in the market.[10–15] Nevertheless, antibodies are isolated from animals or have to be engineered recombinantly and ADCs could suffer from off-target toxicity due to instability of linkers.[16] Targeting peptides, on the other hand, can be prepared in large scale synthetically, bind to a broad range of biological targets, exhibit low toxicity, and possess chemical diversity as well as high potency/selectivity. However, due to the low molecular weight of individual peptides, their application can be limited by short half-life and rapid clearance.[17,18] To overcome the Achilles' heel of peptide therapeutics, nanoparticles formulation with peptides have

M. Raabe, A. J. Heck, S. Führer, D. Schauenburg, M. Pieszka, M. M. Zegota, L. Nuhn, D. Y. W. Ng, S. L. Kuan, T. Weil
Synthesis of Macromolecules
Max Planck Institute for Polymer Research
Ackermannweg 10, Mainz 55128, Germany
E-mail: kuan@mpip-mainz.mpg.de; weil@mpip-mainz.mpg.de

The ORCID identification number(s) for the author(s) of this article can be found under https://doi.org/10.1002/mabi.202100299

DOI: 10.1002/mabi.202100299

M. Raabe, M. Pieszka, T. Wang, M. M. Zegota, S. L. Kuan, T. Weil
Institute of Inorganic Chemistry I
Ulm University
Albert-Einstein-Allee 11, Ulm 89081, Germany

M. Raabe
Department of Synthetic Chemistry and Biological Chemistry, Graduate School of Engineering
Kyoto University
Katsura, Nishikyo-ku, Kyoto 615-8510, Japan

T. Wang
Institute of Urban Agriculture
Chinese Academy of Agricultural Sciences
Chengdu 600213, P. R. China

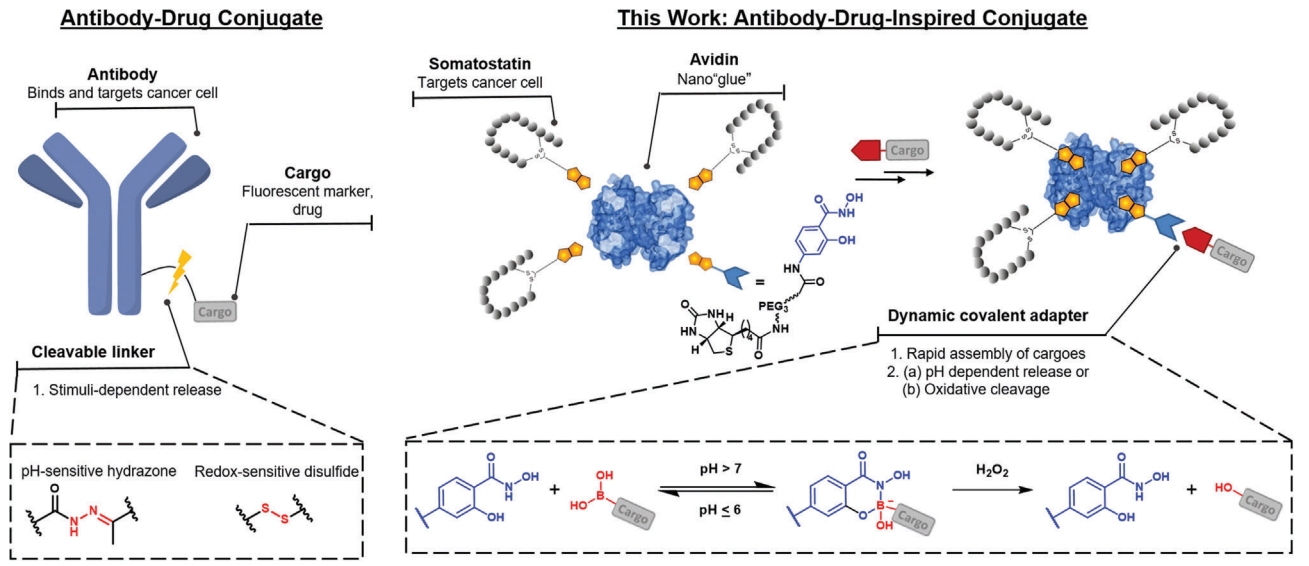

Figure 1. Illustration of the key components and features of the design of an antibody-drug conjugate and an antibody-drug-inspired conjugate that 1) can address receptors overexpressed on cancer cells in a multivalent fashion to achieve internalization and 2) can control release of molecular cargoes via a dynamic covalent linker that is pH-responsive or undergoes oxidative cleavage.

been devised but they are usually considerably larger, lack molecular precision, and require biodegradability into nontoxic metabolites.[19] In this regards, we have previously established the assembly of multiprotein complexes that contain functional proteins as well as multiple copies of targeting peptides on an avidin to target cancer cells that overexpress somatostatin 2 receptors (SSTR2).[20–22] The chemically engineered fusion protein has shown significant improvement for cell-type selective antitumor treatment compared to treatment with the antibody, avastin.[20]

Hence, the preparation of structurally defined AD-inspired conjugates combining multiple targeting groups as well as drug molecules connected by stimulus responsive linkers would offer several advantages. For instance, they could be optimized through synthetic chemistry to provide cell recognition with improved drug potency and through the design of a stable linkage in blood circulation, release the drug payload in the microenvironment at the tumor site.[9,23] In this regards, dynamic covalent chemistry (DCvC) offers many attractive properties since it combines dynamicity of supramolecular chemistry and stability of covalent bonds, and is stimuli responsive.[24–27] The most classical example is the hydrazone linkage, which is often incorporated into delivery platform as a pH-cleavable trigger but is nonreversible due to its slow association rate.[28,29] Moreover, the slow reaction rate of hydrazone formation means that in situ generation of protein-drug conjugate is not feasible. Consequently, other pH-responsive DCv linkers such as the dynamic B–O/N bonds with faster association rates have emerged.[27,30,31] Recent findings have shown that the reactions of boronic acid derivatives with 1,2-diols or the salicylhydroxamic acid (SHA) offer advantages for protein conjugation, namely mild conditions, possibility of using water as a solvent, and pH responsiveness of the resultant B–O and B–N bonds.[32,33] The fast association rates of these interactions also allowed for rapid, in situ assembly of dynamic protein-drug conjugates.[34] In addition, peroxide-triggered cleavage of the boronic acid can also induce release in cancer cells where high concentrations of hydrogen peroxide (H_2O_2) is a hallmark of the tumor microenvironment.[35]

We report herein the design and rapid assembly of an antibody-drug-inspired supramolecular conjugate combining receptor-targeting somatostatin peptides and the drug doxorubicin (DOX) connected with a pH-responsive adapter to mimic key features in ADCs (**Figure 1**). The multipartite conjugate exhibits distinct features at individual domain: 1) recognition sites that allow multiple interactions with cell surface receptor and are arranged 2) on distinct locations on a high molecular weight protein scaffold, 3) a pH-responsive and oxidation-sensitive linker, and 4) a cytotoxic drug molecule. These conjugates target cancer cells overexpressing somatostatin receptors with the possibility for controlled release of the cytotoxic drug in the acidic tumor microenvironment or under oxidative conditions, as well as exhibit stability in biological media.

2. Results and Discussion

2.1. Chemical Design and Synthesis

To prepare a stimuli-responsive trivalent protein-drug conjugate that possesses similar features to ADCs for targeted delivery, three components are required: 1) a dynamic covalent adapter to bridge the avidin carrier and cargo in a pH-dependent manner; 2) boronic acid modified drug or dyes as molecular cargo; and 3) the cyclic peptide, somatostatin, monofunctionalized with biotin to confer cell-type specificity to the conjugate (Figure 1).

To assemble and disassemble the cargo in a pH-responsive fashion, we selected the pH-reversible interaction between boronic acid–salicylhydroxamate (SHA). A bifunctional linker comprising of biotin and SHA was designed and synthesized. We started the synthesis of the biotin–SHA linker with a triethylene glycol chain, for both improved water solubility as well as sufficient spacer length to enable optimal binding to the biotin

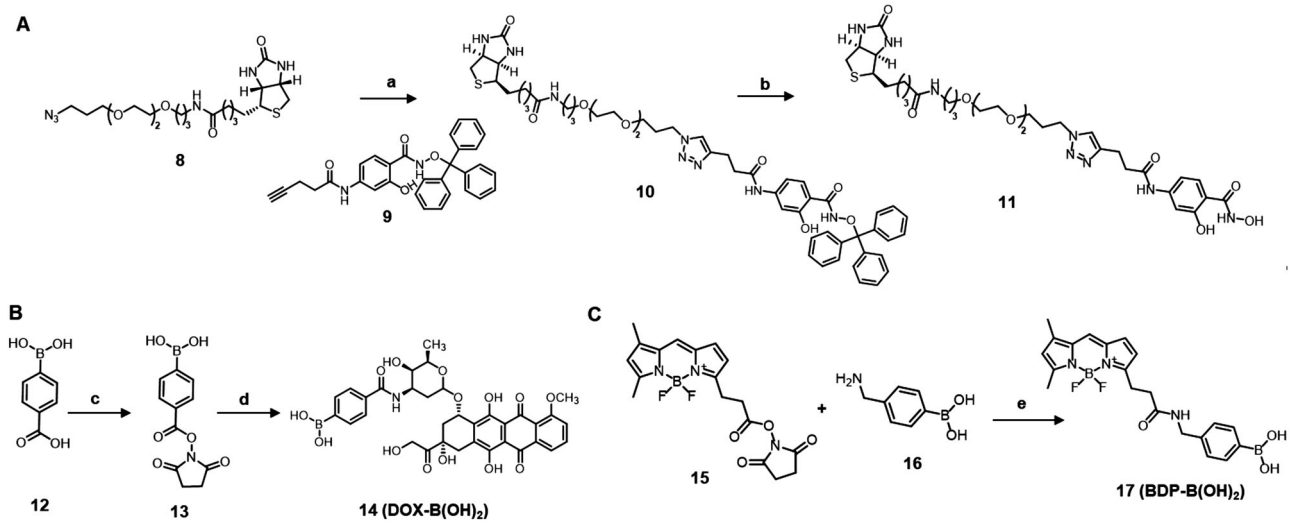

Scheme 1. A) Two steps synthesis of biotin–SHA (compound **11**) from compound **8**; a) **9**, $CuSO_4.5H_2O$, sodium ascorbate, tetrahydrofuran/Milli-Q, room temperature, overnight, quantitative yield; b) triisopropyl silane, trifluoroacetic acid, methanol, room temperature, 2 h, quantitative yield. B) Synthesis of DOX-$B(OH)_2$ (compound **14**), 22% yield; c) NHS, EDC.HCl, DMAP, DMF, room temperature, overnight; d) DOX*HCl, $NaCO_3$, ACN, H_2O, room temperature, overnight, 22% yield. C) Synthesis of BDP-$B(OH)_2$ (compound **17**), 44% yield; e) DMF, DIEA, room temperature, overnight, 44% yield.

binding pocket and the boronic acid modified compounds.[36] The overall synthesis route starting from compound **1** is depicted in the Scheme S1, Supporting Information. The syntheses of precursor compounds **1**–**8** were accomplished using previously reported protocols (Scheme S1, Supporting Information)[37,38] and the critical steps of the synthesis (compounds **10**–**11**) are shown in **Scheme 1**A.

All intermediate compounds were characterized by ^{1}H-NMR and/or ^{13}C-NMR (see Supporting Information). A trityl-protected ethynyl SHA (compound **9**)[37] was coupled to compound **8** by copper catalyzed azide-alkyne cycloaddition to afford compound **10** in quantitative yield. Compounds **8** and **10** were analyzed by liquid chromatography-mass spectrometry (LC-MS, see Figures S3 and S4, Supporting Information) to determine their purity. The target compound **11** (biotin–SHA) was obtained through the deprotection of the trityl group under acidic conditions in quantitative yield. Compound **11** was characterized by ^{1}H-, ^{13}C-NMR, COSY-45, and LC-MS (Figures S1, S2, and S5, Supporting Information). Based on the COSY-45 measurement, all peaks in ^{1}H-NMR could be assigned to the corresponding hydrogen atoms of biotin–SHA (Figure S1, Supporting Information). The chromatogram of the LC-MS revealed at 214 and 254 nm only a single peak with m/z 721 $[M]^+$ and 743 $[M - H + Na]^+$, which is consistent with the calculated mass of compound **11** (calcd. mass: 721 g mol^{-1}, formula $C_{32}H_{48}N_8O_9S$).

In the next step, we synthesized boronic acid functionalized cargoes, which can be bound to the SHA linker **11**. To enable dynamic covalent binding of a drug to the SHA linker, we modified the chemotherapeutic DOX, a known and marketed cytostatic, with a boronic acid group (compound **13**) to yield DOX-$B(OH)_2$ (compound **14**, see Scheme 1B). A carboxyphenylboronic acid (compound **12**) was activated with *N*-hydroxysuccinimide (NHS) to form compound **13** and afterward to react in a condensation reaction with the amine of DOX. Compound **14** was purified by HPLC (22% yield) and further characterized by ^{1}H NMR and LC-MS (Figures S6 and S7, Supporting Information). The chromatogram at 214 nm revealed a single peak and the masses: m/z = 969 [M + acetal fragment (278)]$^+$, 709 [M + H_2O]$^+$, 397, 278 [Acetal fragmentation]$^+$; 690 $[M - H]^-$ (calc. [M]: 691.21 g mol^{-1}), corresponding to compound **14** (Figure S7, Supporting Information). Boronic acid modified dyes, namely BODIPY and rhodamine B were prepared as molecular cargoes. An NHS ester of the BODIPY (BDP, compound **15**) dye was reacted with (4-(aminomethyl)phenyl)boronic acid (compound **16**) to yield BDP-$B(OH)_2$ (compound **17**, 44% yield, see Scheme 1C). BDP-$B(OH)_2$ was characterized by ^{1}H-NMR and LC-MS (Figures S8 and S9, Supporting Information). The chromatogram at 254 nm revealed a single peak and the corresponding masses: m/z = 406.19 [M-HF + H]$^+$, 448.17 [M + Na]$^+$, 489.21 [M + ACN + Na]$^+$, 851.39 [2M + H]$^+$, and 873.37 [2M + Na]$^+$ (Figure S9, Supporting Information). Rhodamine dye was modified with a boronic acid group (Rho-$B(OH)_2$) according to a previous protocol.[39] In addition, a noncleavable Bt–DOX (**18**) was prepared as a control for subsequent cytotoxicity studies (Figures S10–S12, Supporting Information).

For the targeting entity, we selected the cyclic peptide hormone somatostatin (SST), which binds to SST receptors overexpressed on cancer cells.[40,41] SST consists of 14 amino acids and a single disulfide which allows incorporation of a single biotin (biotin-SST).[42] Specifically, a bis-sulfone-based reagent was used and via subsequent Michael additions, disulfide rebridging was accomplished to introduce a single biotin functionality.[37] The reagent was chosen as it was reported that the rebridging allows the site and receptor binding of SST to SSTR2 to be retained.[37]

2.2. Preparation of Somatostatin–Avidin Complex

The multidomain protein constructs were assembled using the avidin–biotin technology through a two-steps process. The

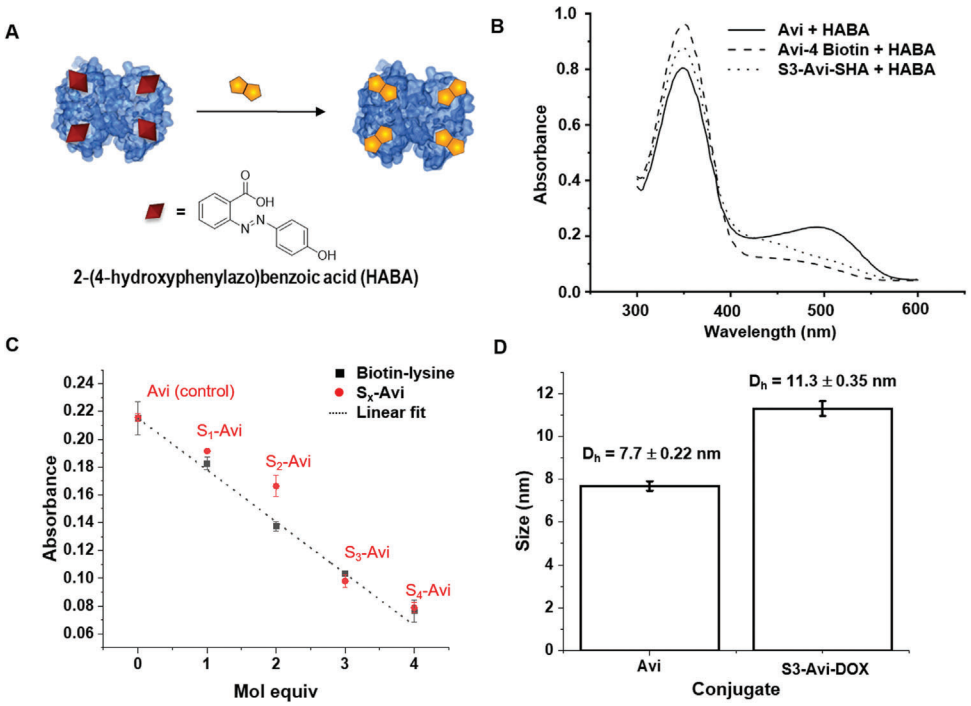

Figure 2. A) Schematic illustration of competitive binding of HABA and biotin to avidin. B) HABA binding assay of Avi, Avi saturated with biotin, and S3-Avi–SHA. C) Linear plot of HABA assay against biotin-lysine ($y = -0.0357x + 0.2144$, $R^2 = 0.9931$) to determine the number of SST per Avi in S1–S4-Avi conjugates. D) Size determination by dynamic light scattering of noncleavable S3-Avi–DOX and Avi.

components used for assembly include avidin, biotin–SHA, boronic acid modified cargoes (BDP-$B(OH)_2$, DOX-$B(OH)_2$, and Rho-$B(OH)_2$), and biotin-SST. Avidin (Avi) is a tetrameric protein of around 66 kDa in size and possesses four natural binding sites for biotin. We adopted a previously reported strategy for the assembly of different ratio of targeting peptides to avidin.[20] First, a competitive binding assay using 2-(4-hydroxyphenylazo)benzoic acid (HABA) with lower binding affinity was used to achieve stoichiometric control (**Figure 2**A).

Because of its higher affinity for avidin, biotin displaces HABA leading to a decrease of absorbance at 500 nm until complete disappearance upon saturation of all binding pockets (Figure 2B). Avidin conjugates with different entities of SST were prepared following the reported method[20] to afford constructs with an average of 0.6 (S1-Avi), 1.3 (S2-Avi), or 3.3 (S3-Avi) SST per avidin. The number of SST per Avi was determined using a linear plot from HABA assay against biotin-lysine (Figure 2C). Thereafter, the empty binding pockets of S1–3-Avi were saturated with a biotin entity to further investigate their binding on cell surfaces expressing SST2 receptors (SSTR2; Figure S13, Supporting Information). Specifically, binding of these conjugates to the SSTR2 and whether this binding is promoted for conjugates with two or three SST per avidin, due to a possible multivalency effect, was studied using an agonistic calcium flux assay offered by Genscript. Serial dilutions of the three conjugates were added to wild type cells (CHO-K1/Gα15) and recombinant cells (CHO-K1/Gα15/SSTR2) overexpressing SSTR2, respectively. The binding of S1–3-Avi conjugates was measured via a fluorimetric assay for calcium flux activation induced upon SSTR2 stimulation and the corresponding results are depicted in Figure S13, Supporting Information. While the wild type showed no binding of S1–3-Avi conjugates, the recombinant cells expressing SSTR2 revealed a concentration-dependent binding of S1–3-Avi conjugates and the half maximum effective concentration (EC_{50}) values, where half of the S1–3-Avi conjugates are bound to the SSTR2 receptor (**Table 1**), were calculated for each conjugate. As expected, a lower EC_{50} value was found for both S2-Avi (137 nM) and S3-Avi (104 nM) conjugates compared to the S1-Avi (371 nM) conjugate (Table 1). The EC_{50} increases by almost threefold in S2-Avi compared to S1-Avi. This observation is likely enhanced due to an additive effect or bivalency. However, the increase in EC_{50} in S3-Avi compared to S2-Avi is less pronounced and is presumably due to the spatial orientation of the peptide and the distribution of the receptors on the cell surface, resulting in a less pronounced increase in binding. Since S3-Avi has the lowest EC_{50} value, further investigations were performed using S3-Avi providing an additional empty binding site for the incorporation of a cargo.

Table 1. The half maximum effective concentration (EC_{50}) values of conjugates with 1–3 somatostatin complexed (S1–S3) to each avidin (Avi) determined by calcium flux assay (Genscript) to measure calcium release induced by the agonistic interactions between SSTR2 and S1–S3-Avi with recombinant CHO-K1 cells overexpressing SSTR2. Samples were obtained in duplicates and measured with concentration range from 0.03 nM–10 μM..

Conjugate	EC_{50}
S1-Avi	371 nM
S2-Avi	137 nM
S3-Avi	104 nM

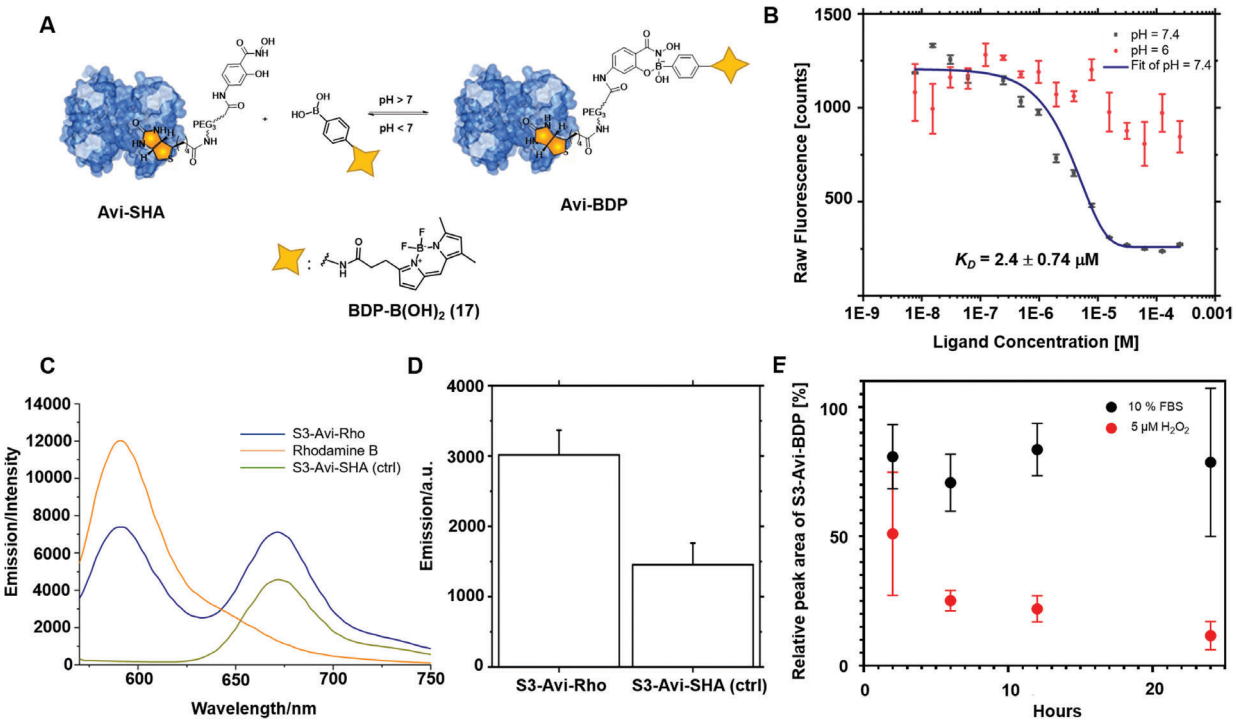

Figure 3. A) Reaction of Avi–SHA and BDP-B(OH)$_2$. B) Fluorescence quenching titration of Avi–SHA against BDP-B(OH)$_2$. A K_D of 2.4 μM was determined at pH 7.4; no binding was observed at pH 6 ($n = 3$, deviation is plotted as SEM). C) Fluorescence emission spectra of 5.8 μM of S3-Avi–Rho, rhodamine B, and S3-Avi–SHA. D) FRET study showing formation of S3-Avi–Rho with S3-Avi–SHA as a control. E) Stability of S3-Avi–BDP in 10% FCS and cargo release under biologically relevant oxidative condition (H_2O_2).

2.3. Preparation of pH Responsive S3-Avi–Cargo, Binding, and Stability Studies

Having determined the EC_{50} of S3-Avi, we proceeded to determine the binding affinity of the Avi–SHA to boronic acid. The pH-dependent binding of Avi–SHA to boronic acid modified probes was investigated using fluorescence quenching, which is observed upon binding of boronic acid to Avi–SHA.[32,33] Serial dilutions of S3-Avi–SHA starting at concentration of 250 μM were titrated to a fixed concentration of 400 nM BDP-B(OH)$_2$ at pH 7.4 or pH 6 and incubated for 30 min (**Figure 3**A). A plot was obtained from the change in fluorescence intensity induced by the binding of Avi–SHA to BDP-B(OH)$_2$ and the K_D was determined to be 2.4 ± 0.74 μM for Avi–BDP (Figure 3B). The result is consistent with previous findings where the SHA–boronic acid interactions are in the low μM range.[43,44] As expected, there was no binding under acidic conditions showing the pH-dependence of the system, which is attractive for the release of molecular cargoes in acidic endolysosomes of cancer cells or in acidic cancer microenvironment.

Next, we proceeded to prepare various pH-responsive S3-Avi–Cargo assemblies (Cargo = DOX, BDP, and Rho). Based on the stoichiometric optimization using HABA, biotin–SHA was added to S3-Avi in the ratio of 1:1 (Figure 2B). The resultant S3-Avi–SHA complex was then incubated with the boronic acid-modified cargo molecules (Figure 3A) to form three different S3-Avi–Cargo complexes. The resultant complexes were purified by ultrafiltration at a MWCO of 10 kDa and characterized by UV–vis (Figure S14, Supporting Information). The identity of the S3-Avi–Cargo was confirmed by the emergence of the characteristic absorbance peak of the respective cargoes (Figure S14, Supporting Information, $\lambda_{BDP} = 509$ nm; $\lambda_{DOX} = 480$ nm). The hydrodynamic diameter of noncleavable S3-Avi–DOX was determined to be 11.3 nm, in comparison to avidin with a diameter of 7.7 nm (Figure 2D and Figure S15, Supporting Information). The size increase is presumably due to the binding of SST to Avi. The binding of S3-Avi–SHA to the boronic acid modified cargoes was further confirmed by Förster resonance energy transfer (FRET), where energy transfer can only occur between two fluorescent entities in close proximity (<10 nm).[45] We selected Cy5 and rhodamine as FRET pair where rhodamine acts as donor and Cy5 as acceptor. For FRET measurements, we statistically labeled Avi with Cy5. Cy5-labeled S3-Avi–SHA and Rho-B(OH)$_2$ were mixed in a ratio of 1:1 and were incubated for 20 min to form S3-Avi–Rho. Cy5-labeled S3-Avi–SHA was implemented as a negative control. Upon excitation at a wavelength of 540 nm, we measured the emission of Cy5 at 672 nm, a significant increase in the emission signal of Cy5-labeled S3-Avi–Rho at 672 nm was observed compared to the control S3-Avi–SHA (Figure 3C,D), suggesting the occurrence of an energy transfer. This confirmed the successful binding of Rho-B(OH)$_2$ to S3-Avi–SHA.

Compared to larger proteins, peptides such as somatostatin could interact with proteins in biological media before reaching targeted sites,[46,47] and linker instability could lead to off-target toxicity, thus hampering applications. Thus, we further investigated the stability of the linker and the supramolecular construct, S3-Avi–BDP (5 μM) in 10% fetal calf serum. Aliquots were drawn after incubation of 2, 6, 12, and 24 h and directly applied and

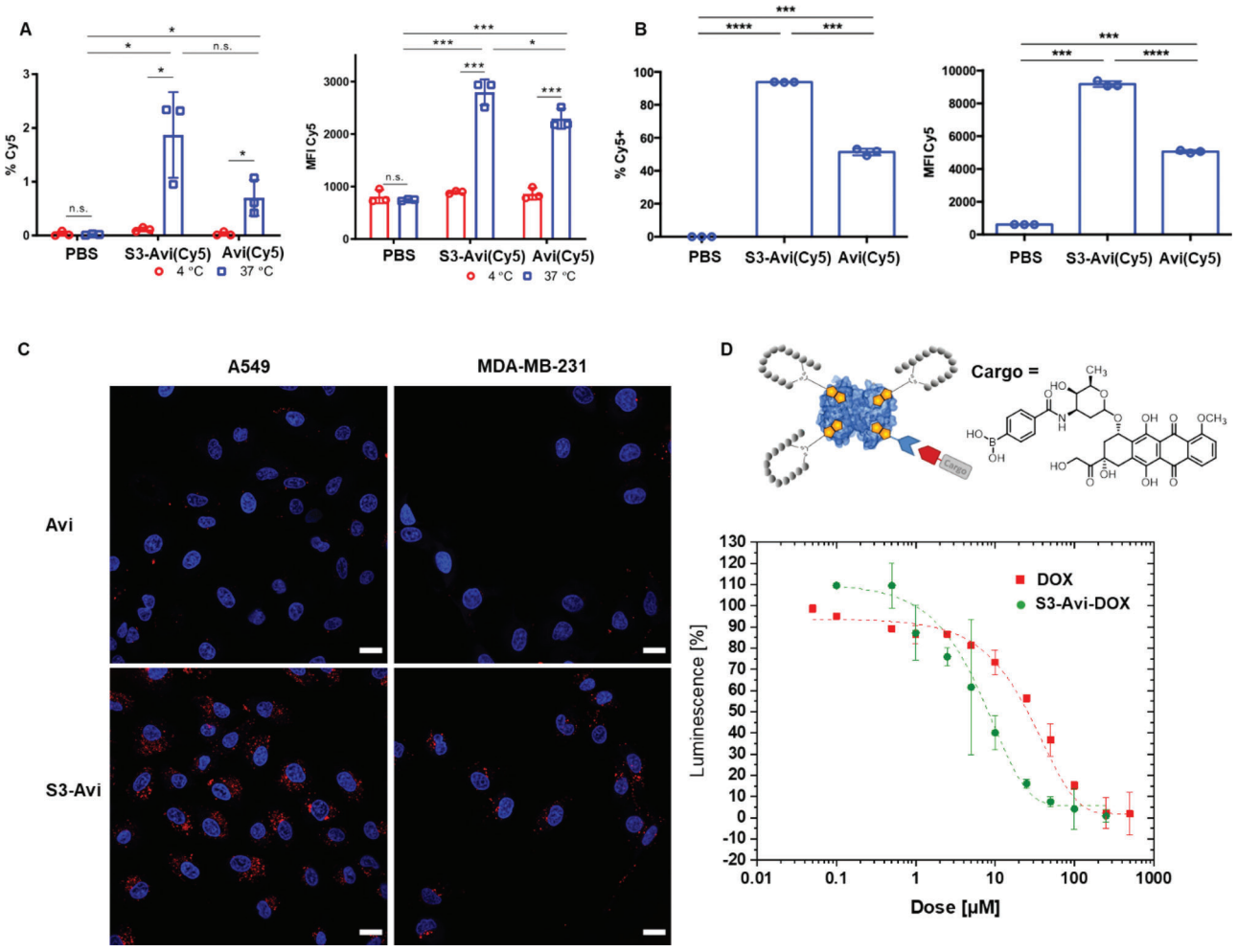

Figure 4. A) Flow cytometry analysis of uptake of S3-Avi into A549 cells at 4 and 37 °C after 30 min incubation ($n = 3$). B) Flow cytometry analysis of uptake of S3-Avi into A549 cells at 37 °C after 4 h incubation ($n = 3$). C) Cellular uptake studies of 500 nM of BDP-labeled S3-Avi and BDP-labeled Avi in A549 lung cancer cells and MDA-MB-231 breast cancer cells after 24 h. Nuclei were stained in blue. Scale bar = 20 μm. D) Cytotoxicity of free DOX versus S3-Avi–DOX in A549 cells ($n = 3$, 250 μM S3-Avi–DOX, $n = 2$).

analyzed using size exclusion chromatography on a fast protein liquid chromatography (FPLC) system with a multiwavelength detector. Remarkably, the construct remained intact up to 24 h, confirming its stability (Figure 3E). Since boronic acid is known to undergo oxidative cleavage to form phenols,[48] we further tested the cleavage of the cargo and its release under biologically relevant concentration of H_2O_2 (5 μM)[49] using FPLC (Figure 3E). At 2 h, there was already a significant decrease in the relative peak area of S3-Avi-BDP by about 49%, indicating the oxidation of S3-Avi–BDP into S3-Avi and free BDP. After 24 h, up to 88% of the S3-Av-BDP had oxidized, suggesting that besides pH, controlled release of the cargo can also be achieved under oxidative conditions found inside cancer cells with neutral extracellular microenvironment.[50]

2.4. Cellular Uptake and Cytotoxicity Studies

SST is an endogenous peptide hormone released through a variety of stimuli and is binding to the membrane's GPCR receptors SSTR1–5. Many solid tumor cell lines, including human lung cancer cell line A549 and breast cancer cell line MDA-MB-231, are overexpressing SSTR2 receptors. Thus, SST has been used for tumor diagnostics and therapeutic purposes. We first verified that SSTR2 is expressed in A549 and MDA-MB-231 cells using western blot (Figure S16, Supporting Information). Since receptor-mediated uptake is an energy-dependent process,[51] the cell uptake of S3-Avi at 4 and 37 °C into the SSTR2-expressing A549 were quantified using flow cytometry. At 4 °C, cell internalization was quenched in both 200 nM of S3-Avi and Avi (control) after 30 min of incubation (**Figure 4**A) but could get more pronounced at 37 °C. After 4 h incubation at 37 °C, the preferred uptake of S3-Avi over the control Avi became more significant compared to 30 min incubation (Figure 4B). Taken together, our results suggest that the internalization of S3-Avi is mostly guided by a receptor-mediated uptake rather than passive diffusion. To further prove the receptor-mediated uptake, we performed studies on BDP-labeled S3-Avi using confocal microscopy with A549 cell line, as well as an additional SSTR2-expressing breast cancer cell line MDA-MB-231 (Figure 4C and Figure S17,

Supporting Information). We found that S3-Avi (500 nM) were internalized into both cell lines in contrast to Avi, which showed no internalization upon incubation at 24 h.

Next, the translocation of a molecular cargo by S3-Avi into A549 cells was confirmed by confocal microscopy using Cy5-labeled S3-Avi–BDP (Figure S18, Supporting Information). Incubation of S3-Avi–BDP (500 nM) for 4 h already showed efficient uptake into A549 using confocal microscopy. Thereafter, the cytotoxicity of a boronic acid modified model drug, DOX (DOX-$B(OH)_2$), was investigated using S3-Avi–DOX. The cytotoxicity and EC_{50} of pH-responsive S3-Avi–DOX toward A549 were determined after incubation for 24 h. S3-Avi–DOX ($EC_{50} = 5 \pm 0.3$ μM, $R^2 = 0.999$) showed significantly reduced cell viability compared to DOX ($EC_{50} = 37 \pm 6$ μM, $R^2 = 0.993$) treatment alone (Figure 4D). There is only a small difference observed compared to treatment with noncleavable S3-Avi–DOX (Figure S19, Supporting Information, $EC_{50} = 27 \pm 17$ μM, $R^2 = 0.954$). The enhancement of EC_{50} of S3-Avi–DOX compared to free DOX is possibly due to more efficient uptake mediated by the S3-Avi platform.

3. Conclusion

In summary, we present a stable, trivalent protein-drug conjugate based on an avidin adaptor platform, which mimics key features of ADCs: 1) cell targeting entity, 2) bioactive cargo, and 3) stable yet responsive linker on a protein scaffold. Moreover, the linker allows facile covalent assembly of cargoes on demand, as demonstrated with three different dyes/drugs. The conjugate is taken up by cancer cells expressing SSTR2 and exhibits stability in biological media. In addition, the assembly of the conjugates capitalizing on the interactions of boronic acid with salicylhydroxamates enabled controlled cargo release in response to pH or oxidative agents. The construct demonstrated enhanced cytotoxicity in SSTR2 receptor overexpressing cell lines compared to the free drug. The results suggest that the system is suitable for assembling cargoes where concentrations in micromolar are sufficient to induce biological effects. For systems where lower cargo dosage is required in submicromolar or nanomolar range, it is possible to increase the binding affinity by adopting a peptide scaffold to introduce multiple interaction points in the linkers.[32] Nevertheless, the platform and chemical strategy presented herein allows the rapid generation of a library of smart protein-drug conjugates and overcome some of the inherent limitations of peptides. We envisage that the reported technology will open new avenues for the innovation of "on-site" conjugation of smart, antibody-drug-inspired conjugates that can respond to various stimuli found inside tumor cells and expands the current repertoire of protein therapeutics beyond classical ADCs.

Supporting Information

Supporting Information is available from the Wiley Online Library or from the author.

Acknowledgements

M.R. and A.J.H. contributed equally to this work. The authors are grateful to the Max Planck Society and the Deutsche Forschungsgemeinschaft (DFG, German Research Foundation) – SFB 1066 (Q05, Project Number 213555243) for the financial support. L.N. acknowledges support by the DFG Emmy Noether Program (Projektnummer 417278389). The authors thank Dr. Matthias Arzt for the ^{13}C-NMR assignment of compound **11** and Dr. Joachim Räder for the HR-ESI-MS measurement of compound **14**.

Open access funding enabled and organized by Projekt DEAL.

Conflict of Interest

The authors declare no conflict of interest.

Data Availability Statement

Data available upon a reasonable request from the author.

Keywords

antibody-inspired conjugates, avidin–biotin, boronic acid–salicylhydroxamate, pH-responsive linkers, protein-drug conjugates

Received: July 28, 2021
Revised: November 11, 2021
Published online: December 4, 2021

[1] B. Leader, Q. J. Baca, D. E. Golan, *Nat. Rev. Drug Discovery* **2008**, *7*, 21.
[2] S. Coats, M. Williams, B. Kebble, R. Dixit, L. Tseng, N.-S. Yao, D. A. Tice, J.-C. Soria, *Clin. Cancer Res.* **2019**, *25*, 5441.
[3] C. D. Spicer, B. G. Davis, *Nat. Commun.* **2014**, *5*, 1.
[4] E. A. Hoyt, P. M. S. D. Cal, B. L. Oliveira, G. J. L. Bernardes, *Nat. Rev. Chem.* **2019**, *3*, 147.
[5] J. M. Chalker, G. J. L. Bernardes, Y. A. Lin, B. G. Davis, *Chem. - Asian J.* **2009**, *4*, 630.
[6] O. Boutureira, G. J. L. Bernardes, *Chem. Rev.* **2015**, *115*, 2174.
[7] N. Krall, F. P. Da Cruz, O. Boutureira, G. J. L. Bernardes, *Nat. Chem.* **2016**, *8*, 103.
[8] A. D. Corso, L. Pignataro, L. Belvisi, C. Gennari, *Chem. - Eur. J.* **2019**, *25*, 14740.
[9] J. D. Bargh, A. Isidro-Llobet, J. S. Parker, D. R. Spring, *Chem. Soc. Rev.* **2019**, *48*, 4361.
[10] S. Sindhwani, A. M. Syed, J. Ngai, B. R. Kingston, L. Maiorino, J. Rothschild, P. MacMillan, Y. Zhang, N. U. Rajesh, T. Hoang, J. L. Y. Wu, S. Wilhelm, A. Zilman, S. Gadde, A. Sulaiman, B. Ouyang, Z. Lin, L. Wang, M. Egeblad, W. C. W. Chan, *Nat. Mater.* **2020**, *19*, 566.
[11] E. Y. Jen, C.-W. Ko, J. E. Lee, P. L. Del Valle, A. Aydanian, C. Jewell, K. J. Norsworthy, D. Przepiorka, L. Nie, J. Liu, C. M. Sheth, M. Shapiro, A. T. Farrell, R. Pazdur, *Clin. Cancer Res.* **2018**, *24*, 3242.
[12] N. C. Richardson, Y. L. Kasamon, H. Chen, R. A. de Claro, J. Ye, G. M. Blumenthal, A. T. Farrell, R. Pazdur, *Oncologist* **2019**, *24*, e180.
[13] L. Amiri-Kordestani, G. M. Blumenthal, Q. C. Xu, L. Zhang, S. W. Tang, L. Ha, W. C. Weinberg, B. Chi, R. Candau-Chacon, P. Hughes, A. M. Russell, S. P. Miksinski, X. H. Chen, W. D. McGuinn, T. Palmby, S. J. Schrieber, Q. Liu, J. Wang, P. Song, N. Mehrotra, L. Skarupa, K. Clouse, A. Al-Hakim, R. Sridhara, A. Ibrahim, R. Justice, R. Pazdur, P. F. D. A. A. Cortazar, *Clin. Cancer Res.* **2014**, *20*, 4436.
[14] Y. N. Lamb, *Drugs* **2017**, *77*, 1603.
[15] D. Al Shaer, O. Al Musaimi, F. Albericio, B. G. de la Torre, *Pharmaceuticals* **2020**, *13*, 40.
[16] M.-R. Nejadmoghaddam, A. Minai-Tehrani, R. Ghahremanzadeh, M. Mahmoudi, R. Dinarvand, A.-H. Zarnani, *Avicenna J. Med. Biotechnol.* **2019**, *11*, 3.

[17] C. Recio, F. Maione, A. J. Iqbal, N. Mascolo, V. De Feo, *Front. Pharmacol.* **2017**, *7*, 526.
[18] S. Muro, *J. Controlled Release* **2012**, *164*, 125.
[19] S. Cao, S. Xu, H. Wang, Y. Ling, J. Dong, R. Xia, X. Sun, *AAPS PharmSciTech* **2019**, *20*, 190.
[20] S. L. Kuan, S. Fischer, S. Hafner, T. Wang, T. Syrovets, W. Liu, Y. Tokura, D. Y. W. Ng, A. Riegger, C. Förtsch, D. Jäger, T. F. E. Barth, T. Simmet, H. Barth, T. Weil, *Adv. Sci.* **2018**, *5*, 1701036.
[21] S. L. Kuan, D. Y. W. Ng, Y. Wu, C. Förtsch, H. Barth, M. Doroshenko, K. Koynov, C. Meier, T. Weil, *J. Am. Chem. Soc.* **2013**, *135*, 17254.
[22] A. J. Heck, T. Ostertag, L. Schnell, S. Fischer, B. K. Agrawalla, P. Winterwerber, E. Wirsching, M. Fauler, M. Frick, S. L. Kuan, T. Weil, H. Barth, *Adv. Healthcare Mater.* **2019**, *8*, 1900665.
[23] Z. Su, D. Xiao, F. Xie, L. Liu, Y. Wang, S. Fan, X. Zhou, S. Li, *Acta Pharm. Sin. B* **2021**, https://doi.org/10.1016/j.apsb.2021.03.042.
[24] A. Wilson, G. Gasparini, S. Matile, *Chem. Soc. Rev.* **2014**, *43*, 1948.
[25] S. J. Rowan, S. J. Cantrill, G. R. L. Cousins, J. K. M. Sanders, J. F. Stoddart, *Angew. Chem., Int. Ed.* **2002**, *41*, 898.
[26] S. Ulrich, *Acc. Chem. Res.* **2019**, *52*, 510.
[27] J. P. M. António, R. Russo, C. P. Carvalho, P. M. S. D. Cal, P. M. P. Gois, *Chem. Soc. Rev.* **2019**, *48*, 3513.
[28] V. T. Bhat, A. M. Caniard, T. Luksch, R. Brenk, D. J. Campopiano, M. F. Greaney, *Nat. Chem.* **2010**, *2*, 490.
[29] E. T. Kool, D.-H. Park, P. Crisalli, *J. Am. Chem. Soc.* **2013**, *135*, 17663.
[30] J. Su, F. Chen, V. L. Cryns, P. B. Messersmith, *J. Am. Chem. Soc.* **2011**, *133*, 11850.
[31] D. Y. W. Ng, M. Arzt, Y. Wu, S. L. Kuan, M. Lamla, T. Weil, *Angew. Chem., Int. Ed.* **2014**, *53*, 324.
[32] M. Hebel, A. Riegger, M. M. Zegota, G. Kizilsavas, J. Gačanin, M. Pieszka, T. Lückerath, J. A. S. Coelho, M. Wagner, P. M. P. Gois, D. Y. W. Ng, T. Weil, *J. Am. Chem. Soc.* **2019**, *141*, 14026.
[33] M. M. Zegota, T. Wang, C. Seidler, D. Y. W. Ng, S. L. Kuan, T. Weil, *Bioconjugate Chem.* **2018**, *29*, 2665.
[34] W. J. Ramsay, H. Bayley, *Angew. Chem., Int. Ed.* **2018**, *57*, 2841.
[35] N. Yang, W. Xiao, X. Song, W. Wang, X. Dong, *Nano-Micro Lett.* **2020**, *12*, 15.
[36] D. S. Wilbur, P. M. Pathare, D. K. Hamlin, S. A. Weerawarna, *Bioconjugate Chem.* **1997**, *8*, 819.
[37] T. Wang, Y. Wu, S. L. Kuan, O. Dumele, M. Lamla, D. Y. W. Ng, M. Arzt, J. Thomas, J. O. Mueller, C. Barner-Kowollik, T. Weil, J. O. Mueller, B.-K. Christopher, T. Weil, *Chem. - Eur. J.* **2015**, *21*, 228.
[38] T. Wang, D. Y. W. Ng, Y. Wu, J. Thomas, T. TamTran, T. Weil, *Chem. Commun.* **2014**, *50*, 1116.
[39] S. Sieste, T. Mack, C. V. Synatschke, C. Schilling, C. M. zu Reckendorf, L. Pendi, S. Harvey, F. S. Ruggeri, T. P. J. Knowles, C. Meier, D. Y. W. Ng, T. Weil, B. Knöll, *Adv. Healthcare Mater.* **2018**, *7*, 1701485.
[40] J. M. Lehman, M. D. Hoeksema, J. Staub, J. Qian, B. Harris, J. C. Callison, J. Miao, C. Shi, R. Eisenberg, H. Chen, S.-C. Chen, P. P. Massion, *Int. J. Cancer* **2019**, *144*, 1104.
[41] F. Barbieri, A. Bajetto, A. Pattarozzi, M. Gatti, R. Würth, S. Thellung, A. Corsaro, V. Villa, M. Nizzari, T. Florio, *Int. J. Pept.* **2013**, *2013*, 926295.
[42] S. Brocchini, S. Balan, A. Godwin, J.-W. Choi, M. Zloh, S. Shaunak, *Nat. Protoc.* **2006**, *1*, 2241.
[43] C. Seidler, M. M. Zegota, M. Raabe, S. L. Kuan, D. Y. W. Ng, T. Weil, *Chem. - Asian J.* **2018**, *13*, 3474.
[44] M. M. Zegota, T. Wang, C. Seidler, D. Y. W. Ng, S. L. Kuan, T. Weil, *Bioconjugate Chem.* **2018**, *29*, 2665.
[45] A. K. Kenworthy, *Methods* **2001**, *24*, 289.
[46] A. G. Harris, *Gut* **1994**, *35*, S1.
[47] P. Dasgupta, R. Mukherjee, *Br. J. Pharmacol.* **2000**, *129*, 101.
[48] M. M. Zegota, M. Müller, B. Lantzberg, G. Kizilsavas, P. Moscariello, M. Martínez-Negro, S. Morsbach, M. Wagner, D. Y. W. Ng, S. L. Kuan, T. Weil, *J. Am. Chem. Soc.* **2021**, *143*, 17057.
[49] M. Pieszka, S. Han, C. Volkmann, R. Graf, I. Lieberwirth, K. Landfester, D. Y. W. Ng, T. Weil, *J. Am. Chem. Soc.* **2020**, *142*, 15780.
[50] G. Hao, Z. P. Xu, L. Li, *RSC Adv.* **2018**, *8*, 22182.
[51] D. Pesce, Y. Wu, A. Kolbe, T. Weil, A. Herrmann, *Biomaterials* **2013**, *34*, 4360.